Available online at www.sciencedirect.com
SCIENCE DIRECT®
Journal of Nuclear Materials 342 (2005) 192–196
journal of nuclear materials
www.elsevier.com/locate/jnucmat

Letter to the Editor

The thermal conductivity and lattice parameter measurements in a low Ce content $(U_{1-y}Ce_y)O_2$ mixed oxide

Dong-Joo Kim [a,b,*], Young-Woo Lee [b], Yong-Soo Kim [a]

[a] Department of Nuclear Engineering, Hanyang University, Seoul 133-791, South Korea
[b] Korea Atomic Energy Research Institute, P.O. Box 150, Yuseong, Daejeon 305-353, South Korea

Received 21 September 2004; accepted 18 March 2005

Abstract

The thermal diffusivities of $(U_{1-y}Ce_y)O_2$ were measured from room temperature to 1673 K using laser flash method, and the lattice parameter was examined as a function of Ce contents using X-ray diffractometry to investigate the theoretical density of each composition. The thermal conductivities normalized to 95% of theoretical density decreased with increasing Ce contents. From the fitting results, it was shown that the increasing CeO_2 content as a solid solution affected the lattice contribution and that the effect of the electron contribution was added at higher Ce content.

PACS: 63.20; 66.70; 44.50; 61.72.D

1. Introduction

The thermal conductivity of nuclear fuel materials is the most important property to evaluate the fuel performance in a nuclear reactor. This property affects the fuel centerline temperature, operating power efficiency, safety, and release of the fission product. In this regard, the thermal conductivities of UO_2 and various doped-UO_2 have been intensively studied by many investigators [1–3].

The importance of cerium and cerium oxide is emphasized as one of the major fission products produced in a nuclear fuel. Further, cerium oxide has often been used as a simulating material for plutonium oxide. Although cerium oxide cannot duplicate the behaviors of plutonium oxide completely, it has been used owing to its similar chemical/thermodynamic behaviors, and a convenience in handling.

In the research of mixed oxide fuel (MOX) using cerium oxide, 20–30 mol% CeO_2 contents are mainly used in the simulation for a fast breeder reactor (FBR) fuel composition, while $UO_2 + CeO_2$ properties data for a low content (below 20 mol%) are required in the relevant research of MOX fuel for pressurized water reactor (PWR).

In the present work, the thermal conductivities were calculated from measured thermal diffusivity using a laser flash method as a function of the Ce contents. For the normalization of the thermal conductivities measured to 95% theoretical density (TD), the lattice parameters and theoretical densities were examined using X-ray diffractometry.

* Corresponding author. Address: Korea Atomic Energy Research Institute, P.O. Box 150, Yuseong, Daejeon 305-353, South Korea. Tel.: +82 42 868 8867; fax: +82 42 868 8868.
E-mail address: djkim@kaeri.re.kr (D.-J. Kim).

0022-3115/$ - see front matter
doi:10.1016/j.jnucmat.2005.03.015

2. Experimental

UO_2 (BNFL, IDR-UO_2) and CeO_2 (Aldrich, 99.9%) powders were mixed with various Ce contents (Ce = 0, 7.63, 14.84, 21.68, 28.17 mol%) using a Turbula^{TM} mixer for 1 h. Then the powder mixtures were milled using a Dynamic Ball Milling Apparatus (DM) for 4 h. Milled powder mixture was compacted with a compaction pressure of 300 MPa and sintered at 2023 K for 4 h in a flowing H_2 atmosphere.

X-ray diffraction peak of a sample was measured by XRD (Mac Science, MAC-M03XHF) using a Cu–Kα target. The step scanning method was used (counting time = 5 sec., step width = 0.05°). Samples for the thermal diffusivity measurement were cut to 0.9–1.1 mm in thickness, 6 mm in diameter from a sintered pellet and polished. In the temperature range between room temperature and 1673 K, the thermal diffusivity was measured using a Laser Flash Apparatus (Netzsch, LFA-427) in a vacuum. Specific heat was calculated from the Neumann-Kopp's law using the literature data of UO_2 and CeO_2 [4–9].

3. Results and discussion

In order to confirm a solid solution formation of the CeO_2 in UO_2 matrix, and to compare it with thermal diffusivities having different Ce contents normalized to 95% of the theoretical density, the X-ray diffraction pattern was measured. Fig. 1 is the X-ray patterns of the specimens with different Ce contents, showing that the measured peak is gradually shifted to the right side. The position of the main peak ((1 1 1) plane) moved from 28.28° of UO_2 toward 28.55° of CeO_2 with increasing Ce contents. Because diffraction peaks near $2\theta = 90°$ are magnified to show the shift more clearly, the peak of (5 1 1) plane was observed (Fig. 2). The calculated lattice parameters from the measured peak data are shown in Fig. 3, and these results were in good agreement with the reference data [10–12]. The following equation was obtained for the relationship between the lattice parameter a in nm and the CeO_2 content [Ce] (mol fraction).

$$a = 0.54695 - 0.00582 \times [\mathrm{Ce}]. \quad (1)$$

The measured lattice parameters were calculated by this equation, and the theoretical densities were obtained by using these results. Table 1 shows that the lattice parameter and theoretical density linearly decreased with increasing Ce contents. It can be considered that CeO_2 in UO_2 matrix is fully formed as a solid solution in this composition range, and also the O/M ratio for these samples is the stoichiometric or the near-stoichiometric state, because the data points are on a straight line, i.e. the measured data follow the Vegard's law. 'Near-stoichiometric state' in these samples does not mean hyper-stoichiometric but hypo-stoichiometric state. In the oxygen potential data in the literature [13,14], it was also shown that the O/M ratio of the samples of similar composition ranges from 2.00 to 1.99, i.e. hypo-near-stoichiometric state.

The thermal conductivity was calculated by using the equation of $k = \alpha_M c_p \rho_M$. The thermal diffusivity, α_M was

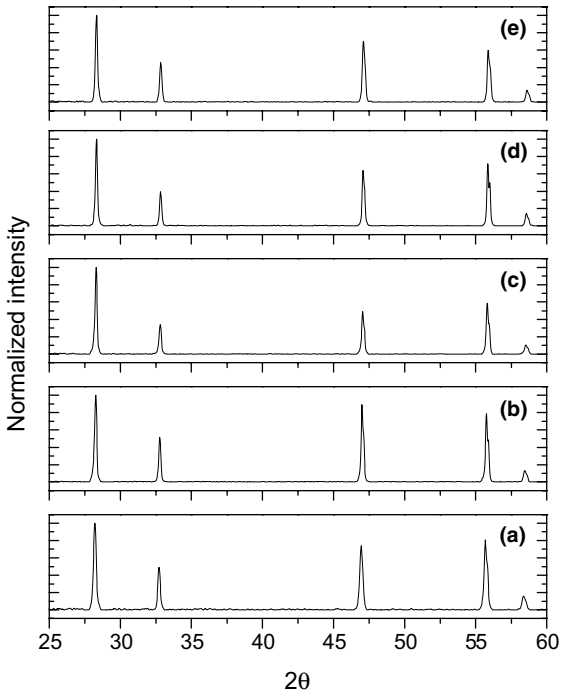

Fig. 1. XRD pattern of the $(U_{1-y}Ce_y)O_2$ samples with the Ce content (mol fraction): (a) $y = 0$, (b) 0.0763, (c) 0.1484, (d) 0.2168 and (e) 0.2817.

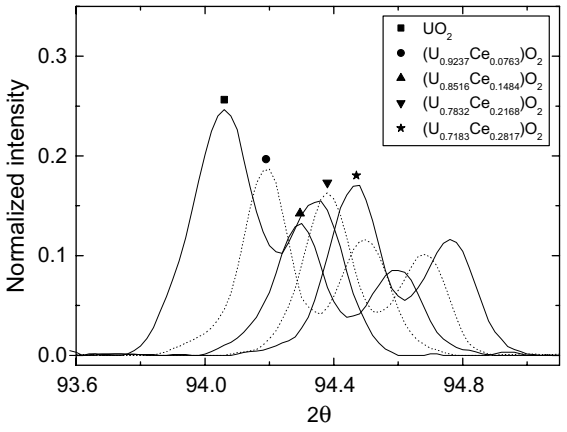

Fig. 2. Extended view of the XRD pattern for UO_2 and $(U,Ce)O_2$ (near 90°).

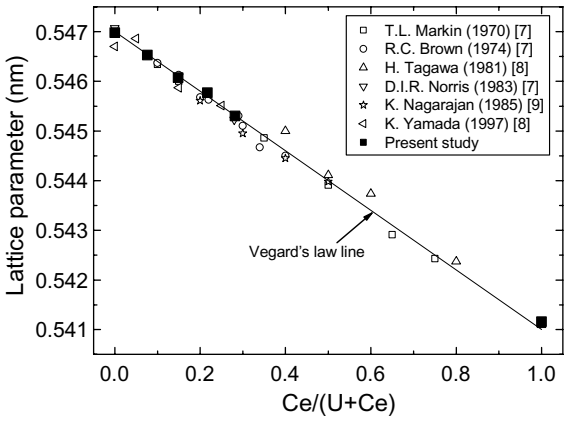

Fig. 3. The measured lattice parameters and literature data of $(U,Ce)O_2$ as a function of the Ce contents.

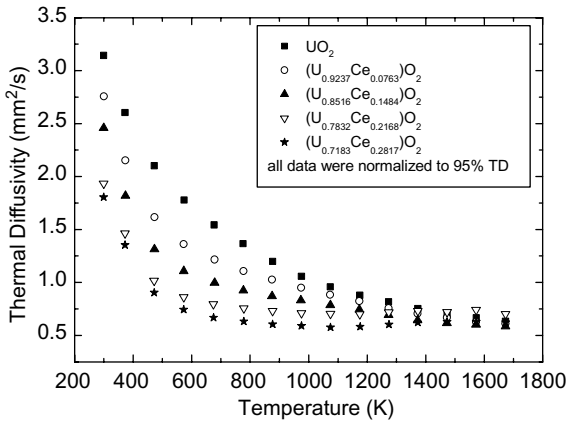

Fig. 4. Thermal diffusivities of $(U_{1-y}Ce_y)O_2$ with varied Ce content as a function of temperature.

measured by using the laser flash method (Fig. 4). The specific heat, c_p, was calculated from Neumann-Kopp's law. All the thermal conductivities were normalized to a 95% theoretical density using the modified Loeb equation [15] and the following expression:

$$K_M = K_{th}(1 - P\eta), \tag{2}$$

$$K_{95} = \frac{K_M(1 - 0.05\eta)}{(1 - P\eta)}, \tag{3}$$

where K_{95} is the thermal conductivity normalized to 95% TD, K_M the thermal conductivity of a sample with a density of ρ_M, P the porosity, η the experimental parameter expressed as $2.6–5 \times 10^{-4}\ T$ [16], and T the temperature for the measurements, in K.

Fig. 5 shows the gradually decreasing thermal conductivities with increasing Ce contents. It is also shown that the thermal conductivities of CE15, CE20 (Table 1) decreased with increasing temperature up to about 973 K, however, slightly increased in the higher temperature region. Similar result was published by Kurosaki [17]. The tendency of the slight increment in the higher temperature region will be explained using the values of C and D among the fitting results as described below.

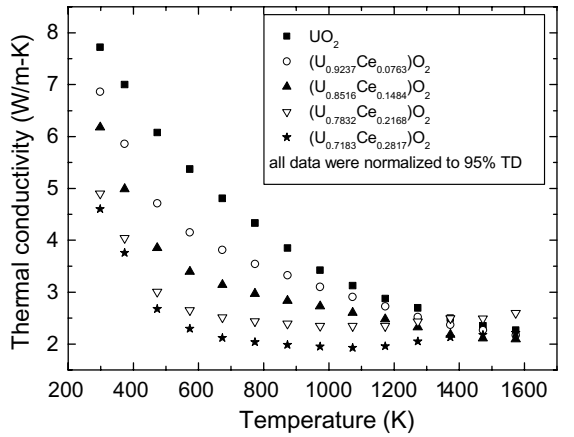

Fig. 5. Thermal conductivities of $(U_{1-y}Ce_y)O_2$ with varied Ce content as a function of temperature.

The thermal conductivity data were fitted using the following relationship [16,17] considered both the lattice and the electron contribution, with a commercial curve fitting program (Origin 7.0, OriginLab^{TM} Co.),

Table 1
Sample compositions, the measured lattice parameters, and the calculated theoretical densities of $(U_{1-y}Ce_y)O_2$ used for the experiments

Sample no.	CeO_2 content		Lattice parameter (nm)		Theoretical density (g/cm^3, 100%TD)
	wt%	mol%	Measured	Calculated	
CE0	0	0	0.54698	0.54695	10.960
CE5	5	7.63	0.54653	0.54651	10.683
CE10	10	14.84	0.54607	0.54610	10.419
CE15	15	21.68	0.54577	0.54570	10.168
CE20	20	28.17	0.54530	0.54532	9.929

Table 2
Calculated values of A, B, C and D of $(U_{1-y}Ce_y)O_2$ from the fitting relationship

Sample no.	Ce content (mol%)	A (m K/W)	B (m/W)	C	D
CE0	0	0.05214	0.00025	–	–
CE5	7.63	0.06600	0.00031	0.00030	363.43
CE10	14.84	0.08836	0.00036	0.00070	1021.52
CE15	21.68	0.20632	0.00032	0.00156	1370.22
CE20	28.17	0.23807	0.00044	0.00171	1433.29

$$k = \frac{1}{A + BT} + CT \exp\left(-\frac{D}{T}\right). \quad (4)$$

Table 2 and Fig. 6 shows the calculated values of A, B, C and D. The parameters of electron contribution, C and D, for UO_2 sample can be negligible, because it is sufficient to describe the thermal conductivity of UO_2 using the lattice contribution only, in the temperature region of this experiment (from room temperature to 1673 K). However, for $(U, Ce)O_2$ samples, the explanation including the electron contribution is needed to describe the thermal conductivity, especially, for the higher Ce content.

First, the following equation is the relationship between A and B, the parameters of lattice contribution [18,19].

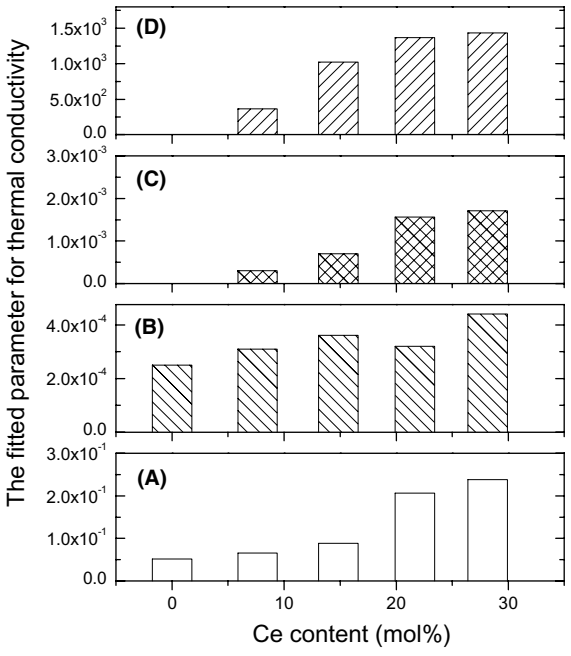

Fig. 6. The fitting values of A, B, C and D as a function of Ce contents.

$$w = \frac{1}{\lambda} = w_l + w_p = A + BT, \quad (5)$$

where w is the thermal resistivity, w_l is the resistivity for the phonon–lattice defect interactions (A), and w_p is for the phonon–phonon interactions (BT). In the case of the mixed oxide, both parameters depend on the two variables, the extent of non-stoichiometry and the additive (Ce) content, simultaneously [20] (not respectively). That is to say, the thermal conductivity of the mixed oxide samples is affected by both A and BT terms at the same time. However, in this experiment, it can be thought that the Ce content is primarily responsible for the thermal conductivity of (U, Ce)O_2, because the O/M ratio of these samples is near-stoichiometric state. From the fitting results, as shown in Fig. 6, the values of A and B increase gradually with increasing Ce contents. It can be concluded that the dissolved Ce atoms substituting U atom in U sub-lattice act as the point defect, which interrupt the transport of heat energy. At last, the thermal conductivity decreases. That is to say, that the increasing content of dissolved CeO_2 affects the phonon–lattice defect interaction. The oxygen vacancy formed during the sintering process in a H_2 atmosphere can also act like a point defect, but it can be said that the influence by the dissolved Ce atoms is dominant, as previously stated, because of the O/M ratio of near-stoichiometry in these samples. Also, the content of the dissolved CeO_2 affects the phonon–phonon interaction (BT). It can be considered that the lattice anharmonicity increased with the increasing mass difference between the additive (Ce) and the host (U) atoms, and this anharmonicity on the lattice vibration affected phonon–phonon scattering [20].

Secondly, Fig. 6 shows that the parameters of electron contribution, C and D in Eq. (4), gradually increased with increasing Ce content, i.e. the effect of electron contribution appeared. This tendency was obscure at lower Ce contents (CE5, CE10), but slightly revealed at higher Ce contents (CE15, CE20). It can be supposed that the electron contribution caused by the higher Ce content affects the thermal conductivity increase at higher temperature, because the concentrations of the electron are increased by the existence of trivalent

Ce ions substituted for U ions [21]. And these electrons act as a carrier for heat conduction.

4. Summary

The thermal diffusivities of $(U_{1-y}Ce_y)O_2$ were measured from the room temperature to 1673 K using the laser flash method, and the lattice parameters were examined using X-ray diffractometry to obtain the theoretical densities of each specimen with different composition.

1. The thermal conductivities normalized to 95% of theoretical density decreased with increasing Ce contents. Exceptionally, the thermal conductivity of the high Ce content samples increased slightly, above about 1000 K.
2. It is concluded that the increasing dissolved CeO_2 in UO_2 matrix causes the lattice contribution to decrease the thermal conductivity of $(U,Ce)O_2$. That is to say, the Ce atom substituting U atom act as a point defect (phonon–lattice defect interaction), and the mass difference between Ce and U atom increases the lattice anharmonicity (phonon–phonon interaction).
3. Especially, for higher Ce content, it can be supposed that the electron contribution in addition to the lattice contribution affected the thermal conductivity of $(U,Ce)O_2$ samples, because the concentrations of the electron are increased by the existence of trivalent Ce ions substituted for U ions. And these electrons act as a carrier for heat conduction.

Acknowledgement

The authors acknowledge that this work has been performed under the Nuclear Mid- and Long-term R & D Projects supported by the Ministry of Science and Technology in Korea. We also would like to thank Dr. J.H. Yang and Mr J.H. Kim of KAERI for their helpful discussions.

References

[1] D.G. Martin, J. Nucl. Mater. 110 (1982) 78.
[2] M. Hirai, S. Ishimoto, J. Nucl. Sci. Technol. 28 (11) (1991) 995.
[3] M.V. Krishnaiah, G. Seenivasan, P. Murti, C.K. Mathews, J. Nucl. Mater. 306 (2002) 10.
[4] Outokumpu HSC chemistry 4.0 for windows, Chemical reaction and equilibrium software with extensive thermochemical database, 1999.
[5] E.H.P. Cordfunke, R.J.M. Konings, Thermochemical Data for Reactor Materials and Fission Products, North Holland, Amsterdam, 1990.
[6] D.L. Hagrman, G.A. Reymann and R.E. Mason, NUREG/CR-0479 TREE-1280, Rev. 2, 1981, p. 1.
[7] J.K. Fink, J. Nucl. Mater. 279 (2000) 1.
[8] J.J. Carbajo, G.L. Yoder, S.G. Popov, V.K. Ivanov, J. Nucl. Mater. 299 (2001) 181.
[9] Y. Arita, T. Matsui, S. Hamada, Thermochim. Acta 253 (1995) 1.
[10] D.I.R. Norris, P. Kay, J. Nucl. Mater. 116 (1983) 184.
[11] K. Yamada, S. Yamanaka, T. Nakagawa, M. Uno, M. Katsura, J. Nucl. Mater. 247 (1997) 289.
[12] K. Nagarajan, R. Saha, R.B. Yadav, S. Rajagopalan, K.V.G. Kutty, M. Saibaba, P.R. Vasudeva Rao, C.K. Mathews, J. Nucl. Mater. 130 (1985) 242.
[13] T. Fujino, J. Nucl. Mater. 154 (1988) 14.
[14] T.L. Markin, E.C. Crouch, J. Inorg. Nucl. Chem. 32 (1970) 77.
[15] A.L. Loeb, J. Am. Ceram. Soc. 37 (1954) 96.
[16] Thermal conductivity and thermal diffusivity of solid UO_2, MATPRO, 1999, http://www.insc.anl.gov/matprop/.
[17] K. Kurosaki, R. Ohshima, M. Uno, S. Yamanaka, K. Yamamoto, T. Namekawa, J. Nucl. Mater. 294 (2001) 193.
[18] R. Brandt, G. Neuer, J. Non-Equilib. Thermodyn. 1 (1976) 3.
[19] C. Duriez, J.P. Alesandri, T. Gervais, Y. Philipponneau, J. Nucl. Mater. 277 (2000) 143.
[20] D.R. Olander, Fundamental aspects of nuclear reactor fuel elements, TID-26711-P1, 1976, 122.
[21] S.H. Kang, J.D. Yi, H.I. Yoo, S.H. Kim, Y.W. Lee, J. Phys. Chem. Solids 63 (2002) 773.